Driver-Free Assessment of Liver Stiffness Using Fast Strain-Encoded (FSENC) MRI

Ahmed A. Harouni[1], Ahmed M. Gharib[2], Nael F. Osman[3], Roderic I. Pettigrew[2], and Khaled Z. Abd-Elmoniem[2]

[1]*Clinical Center, National Institutes of Health, Bethesda, Maryland, United States,* [2]*NIDDK, National Institutes of Health, Bethesda, Maryland, United States,* [3]*Russell H. Morgan Department of Radiology, Johns Hopkins University School of Medicine, Baltimore, Maryland, United States*

INTRODUCTION: Liver cirrhosis, the last stage of fibrosis, is the sixth leading cause of death in high-income countries [1]. Recent research has shown that liver fibrosis is reversible in early stages [2]. Therefore, there is a need for early detection of liver fibroses. Biopsy is the gold standard for determining fibrotic stage. However, biopsy is subjective to a small liver sample and may be subjective to different pathological interpretation. MR elastography (MRE) has emerged as an effective non-invasive procedure to detect liver fibrosis in early stages. Typically, this requires an external driver to pulse the liver. In this work, we propose to use the myocardium's intrinsic motion as a source of vibration with fast strain-encoded (FSENC) MRI[4] to measure the strain through the liver's left lobe adjacent to the myocardium. Unlike traditional MRE [3], FSENC uses intrinsic cardiac motion, is fast (requires one breath hold), and uses simple post-processing performed at the scanner console.

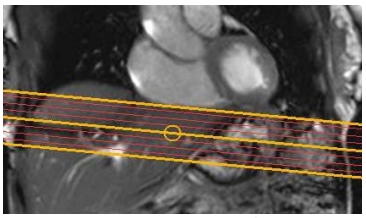

Fig.1: Coronal SSFP image for a healthy subject showing tilted axial image planes used for T1W and FSENC images.

METHODS: As the myocardium contracts during systole, it pulls the left lobe of the liver thus resulting in positive strain, which can be quantified using FSENC, thus separating healthy soft liver from stiff fibrotic liver.

Phantom experiments were designed to test and validate our technique. Three homogenous phantoms composed of water, Agar, and different beef gelatin concentrations were constructed to simulate livers with different stiffness. Hardware similar to the one described by Harouni *et al.* [5] was used to simulate cardiac cyclic motion pushing the liver phantom. During the first half of the cycle a compressing piston moves away allowing the phantom to stretch thus yielding in a positive strain, while in the second half of the cycle the piston compresses the phantom to initial position. The hardware was designed to simulate heart rates of 55 beat per minute with maximum strain of 15%.

In vivo experiments included nine healthy subjects with no history of liver disease and two patients with diffuse liver disease who signed the informed consent forms and were scanned at a tilted imaging plane parallel to the heart-liver interface (see Fig.1),

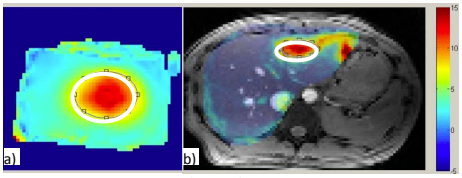

Fig.2: Marker image for soft phantom (a) and healthy subject (b) with automatically selected ROI.

MRI scans were performed at a 3T MRI Philips scanner (Achieva, Philips Medical Systems, Best, the Netherlands) using a 32-channel phased array cardiac-abdominal coil. MRI sequences included coronal SSFP sequence (TR/TE= 2500/60 ms, field-of-view (FOV)= 340x340 mm^2, slice thickness (ST)= 5 mm, temporal resolution= 10 ms); Axial T1W sequence (TR/TE= 3.6/1.24 ms, FOV= 340x340 mm^2, in-plane resolution of 1x1 mm^2, 20 slices, ST= 5mm); FSENC sequence (TR/TE= 7.5/1.1 ms, FOV= 340x340 mm^2, in-plane resolution of 5x5 mm^2, 7 slices, ST= 9 mm, gap= -3 mm, last flip angle= 30°, spiral K-space acquisition= 6 ms, TFE factor= 3, temporal resolution= 30 ms. Tagging, and low and high tunes special frequencies were 0.96 mm $^{-1}$, 0.91 mm^{-1}, and 0.97 mm $^{-1}$, respectively). FSENC scan was performed every other heart beat to allow magnetization to fully recover. FSENC was scanned in one 14 sec breath-hold. Fig.1 shows tilted axial images used for T1W and FSENC scans.

DATA ANALYSIS: Coronal SSFP images along with T1W images were used to determine slices of liver sections immediately below the myocardium. Liver through-plane strain was calculated from FSENC images throughout the cardiac cycle. An elliptical region of interest (ROI) was used to calculate average strain throughout time for each slice. In order to determine the parameters of the ROI, a marker image was generated as the spatial and temporal average of the strain maps of all frames acquired during systole. The point of peak strain in the marker image was chosen as the center of a two-dimensional Gaussian surface to fit the localized strain pattern in the marker image. The Gaussian fit then determines the center of the elliptical ROI as well as the major and minor axes, which are set to full width half maximum of strain. Fig. 2 shows marker strain image for soft phantom (a) and healthy subject (b) along with the automatically selected ROI. Peak strain for healthy subjects and patients were compared using single tail student t-test. Two tailed student t-test was used to compare peak strain for repeated exams for the three healthy subjects.

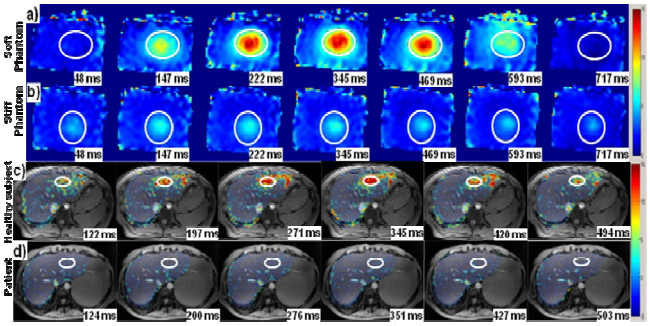

Fig. 3: Strain images for soft phantom (a) stiff phantom (b) Healthy subject (c) and patient (d) throughout time along with automatically selected ROI.

RESULTS: Fig. 3a,b) shows strain images for soft and stiff phantoms, respectively, along with the automatically selected ROI. Fig. 4a shows strain curves for the three phantoms throughout the compression cycle. Soft phantom yields in higher peak strain (10.3%) than medium (8.5%) and stiff phantoms (4.0%). Fig. 3c,d shows liver strain images overlaid over T1W images for a healthy subject and a patient, respectively, throughout the cardiac cycle. Healthy liver yields a high positive strain (>10%) for all slices where as diseased liver yields low strain values (<6%) over all slices. Fig. 4b shows strain curves for two healthy subjects (solid curves) and two patients (broken curves). Peak strain was 13.5%±0.86% (range 12.3%-14.5%) and 4.35±2.88 (range 2.3%-6.4%) for healthy subjects and patients, respectively. Peak strain measured in healthy subjects was significantly ($p<0.0001$) higher than in patients. High correlation between the measurements from the repeated scans of the three subjects (R=0.93, slope 0.94, intersect 0.27). Two tailed paired student t-test showed no significant difference (P=0.73) between repeated strain measurements for healthy subjects.

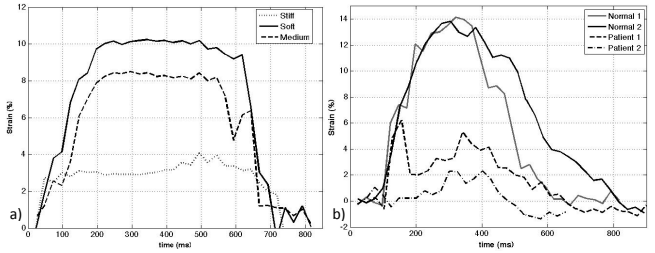

Fig.4: Strain curves for phantom (a) and in-vivo (b) experiments.

CONCLUSION: In this work, we presented a new non-invasive, fast, and simple method to asses liver stiffness using FSENC MRI. Our results showed significant difference between peak strain measured for healthy subjects and patients. Future improvements may include increasing temporal resolution in order to capture the strain pull-up slope as the myocardium is contracting. Also we may consider using slice following FSENC to overcome the through plan motion artifacts. Further work is needed to determine the sensitivity of SENC as an early liver fibrosis detector. Further research should consider large population of patients at different fibrotic stages. Unlike liver biopsy that is invasive and restricted to a small sample size, FSENC MRI is a non-invasive method. FSENC is easy to implement since it relies on the cardiac induced motion to deform the liver with no external device. Thus, it would be immediately implemented on conventional MRI systems. Moreover, since it only requires one breath-hold and does not require complicated post processing software, it could be simply added to current abdominal scans.

REFERENCES: [1] Oxford Univ Press, USA, 2006. [2] Ann Intern Med, 127(11) p.981-5, 1997. [3] Radiology, 240(2) p.440-8, 2006. [4] MRM, 55(2) p.386-95, 2006. [5] Acad Radiol, 18(6) p.705-15, 2011.